



## Molecular Crystals and Liquid Crystals Science and Technology. Section A. Molecular Crystals and Liquid Crystals

Publication details, including instructions for authors and subscription information:

<http://www.tandfonline.com/loi/gmcl19>

### Wavelength Dependence of Scattering in PDLC Films: Droplet Size Effects

Jack Kelly<sup>a</sup>, Wei Wu<sup>a</sup> & Peter Palffy-muhoray<sup>a</sup>

<sup>a</sup> Department of Physics and Liquid Crystal, Institute, Kent State University, Kent, OH, 44242

Version of record first published: 04 Oct 2006.

To cite this article: Jack Kelly, Wei Wu & Peter Palffy-muhoray (1992): Wavelength Dependence of Scattering in PDLC Films: Droplet Size Effects, *Molecular Crystals and Liquid Crystals Science and Technology. Section A. Molecular Crystals and Liquid Crystals*, 223:1, 251-261

To link to this article: <http://dx.doi.org/10.1080/15421409208048256>

PLEASE SCROLL DOWN FOR ARTICLE

Full terms and conditions of use: <http://www.tandfonline.com/page/terms-and-conditions>

This article may be used for research, teaching, and private study purposes. Any substantial or systematic reproduction, redistribution, reselling, loan, sub-licensing, systematic supply, or distribution in any form to anyone is expressly forbidden.

The publisher does not give any warranty express or implied or make any representation that the contents will be complete or accurate or up to date. The accuracy of any instructions, formulae, and drug doses should be independently verified with primary sources. The publisher shall not be liable for any loss, actions, claims, proceedings, demand, or costs or damages whatsoever or howsoever caused arising directly or indirectly in connection with or arising out of the use of this material.

## WAVELENGTH DEPENDENCE OF SCATTERING IN PDLC FILMS: DROPLET SIZE EFFECTS

JACK KELLY, WEI WU, AND PETER PALFFY-MUHORAY  
Department of Physics and Liquid Crystal Institute, Kent State University,  
Kent OH 44242

(Received December 12, 1991)

**Abstract:** We have measured the optical transmittance of UV-cured epoxy PDLC films at normal incidence as a function of applied voltage for a number of different wavelengths. By controlling the cure rate of each film, we were able to study a range of droplet sizes from approximately 0.5 microns to 2.5 microns. By assuming a simple exponential decay law for the transmitted intensity, we have extracted the wavelength dependence of the effective droplet scattering cross-section. This cross-section depends strongly on both the applied voltage and the droplet size. We compare the results with a model based on the anomalous diffraction description of the scattering and find good quantitative agreement.

### INTRODUCTION

PDLC films consist of micron-sized, spheroidal inclusions (droplets) of liquid crystal imbedded in a polymer matrix. These films can be switched from a highly scattering state to a highly transmissive one through the application of an external field. It is of great practical interest to understand this scattering in some detail. One expects that the scattering will be strongly dependent on droplet size and the wavelength of the incident light.

Zumer<sup>1,2</sup> has theoretically studied the scattering of light from isolated spherical birefringent droplets. The scattering falls into two regimes: droplets much smaller than a wavelength of the incident radiation, where the Rayleigh-Gans approximation may be applied<sup>1</sup>, and droplets comparable to the wavelength, where the anomalous diffraction (AD) approach is valid<sup>2</sup>. Little work has been done on applying these single-droplet results to the study of films with a high density of scatterers where the droplets are clearly not isolated. Understanding the distribution of scattered intensity is difficult because of multiple scattering events and lack of detailed knowledge regarding the distribution of the droplets. However, the transmitted intensity is much less sensitive to these effects. In the case of Rayleigh-Gans scattering, the transmitted intensity has been verified to obey a simple exponential decay law with the droplet scattering cross-section varying inversely as the fourth power of the wavelength<sup>3</sup>. No similar work has been carried out for the more technologically important case of AD scattering.

Here we investigate the wavelength dependence of scattering in PDLC films for different droplet sizes and different applied fields in the AD regime. In fact, we will only be concerned with the transmittance and not the angular distribution of the scattered intensity.

### MODELLING THE SCATTERING

The intensity of a beam of light traversing a PDLC film will be attenuated as the light is scattered out of the beam by the liquid crystal droplets. We presume that the attenuation of the initial intensity,  $I_0$ , follows an exponential decay law:

$$I = I_0 e^{-\rho \sigma d} \quad (1)$$

$I$  is the beam intensity after traversing a film of thickness,  $d$ ;  $\rho$  is the droplet density and  $\sigma$  is the film-averaged droplet cross-section. To obtain an expression for this cross-section, we start with the AD cross-section of a droplet with uniform director configuration whose droplet director  $\mathbf{N}$  makes an angle  $\theta$  with the incident wavevector  $\mathbf{k}$  ( $|\mathbf{k}| = k$ ):<sup>2</sup>

$$\sigma_s(\theta, \phi) = 2\sigma_o \cos^2 \phi \left[ 1 - \frac{2}{\nu} \sin(\nu) + \frac{2}{\nu^2} (1 - \cos(\nu)) \right] , \quad (2)$$

where  $\sigma_o = \pi R^2$  is the geometrical cross-section of the spherical droplet of radius  $R$ ; and, to lowest order in the liquid crystal birefringence,  $\Delta n$ ,

$$\nu = 2\Delta n k R \sin^2(\theta) . \quad (3)$$

To obtain this form for  $\nu$  matching of the polymer refractive index and the ordinary index of the liquid crystal is assumed; this is approximately valid for most PDLC systems of interest. The angle  $\phi$  in Equation 2 is the angle that the electric vector of the incident wave makes with the plane defined by  $\mathbf{N}$  and  $\mathbf{k}$ .

The average total cross-section is

$$\sigma = \int_{\Omega} \sigma_s(\theta, \phi) \rho_s(\Omega) d\Omega \quad (4)$$

$\rho_s(\Omega)$  is the density of droplet directors in the in the solid angle  $d\Omega$ . In the absence of an external field we assume that the droplet directors are randomly oriented, i.e.  $\rho_s(\Omega) = \frac{1}{4\pi}$ . Under the influence of an applied field, the directors

reorient toward the direction of the field, altering the distribution. This distribution function has been evaluated by modelling the droplets as identical ellipsoids of revolution whose major axes are randomly oriented.<sup>4,5</sup> The uniform distribution in the azimuthal angle  $\phi$  is unaltered by the field. By balancing the field and elastic torques on each droplet, the angle  $\theta$  in the presence of the field can be expressed in terms of the corresponding equilibrium angle,  $\alpha$ , without the field:

$$\cos^2(\theta) = \frac{1}{2} + \frac{1}{2} \frac{e^2 - 1 + 2\cos^2\alpha}{\sqrt{(e^2 - 1)^2 + 4e^2\cos^2\alpha}} . \quad (5)$$

Here  $e$  is a dimensionless electric field proportional to the external field  $E$  that includes depolarizing effects of the film<sup>4</sup>.  $\alpha$  is the angle that the major axis of the ellipsoid makes with the applied field. For randomly oriented ellipsoids, the distribution of  $\alpha$  is:

$$\rho(\alpha) = \sin(\alpha) \quad : \quad 0 < \alpha < \frac{\pi}{2}. \quad (6)$$

There is no physical distinction between angles less than  $90^\circ$  and those greater than  $90^\circ$ , hence the restriction on  $\alpha$ . It is easier to evaluate Equation 4 with the distribution  $\rho(\alpha)$  rather than  $\rho(\theta)$ . This is done by treating  $\sigma_s(\theta, \phi)$  as an implicit function of  $\alpha$  through Equations 3 and 5:

$$\sigma = \frac{1}{2\pi} \int_{\alpha} \int_{\phi} \sigma_s[\theta(\alpha), \phi] \cdot \sin(\alpha) d\alpha d\phi . \quad (7)$$

It is possible to evaluate the total film cross-section as a function of  $kR$  numerically from Equation 7 for different external fields  $e$  (Figure 1). The birefringence of E7 at room temperature ( $\Delta n = 0.225$ ) was used for the calculations. Note that the cross-section is normalized to the geometrical cross-section.

According to the model, in the absence of an applied field, the behavior of the normalized cross-section,  $\sigma/\sigma_o$ , is quadratic in  $kR$  for small  $kR$ . The cross-section above  $kR \approx 13$  oscillates in the vicinity of the geometrical cross-section. As a field is applied, this oscillatory behavior is suppressed; the principal maximum in the cross-section vanishes first, with subsequent maxima vanishing at successively higher fields. For sufficiently high fields, the quadratic dependence of the normalized cross-section on  $kR$  that is present at small  $kR$  dominates any region of  $kR$ .

A sample order parameter which indicates the degree of droplet director realignment under the influence of the field can be defined:

$$S_s = \frac{1}{2} \langle 3 \cos^2 \theta - 1 \rangle_{\text{sample}} . \quad (8)$$

For a random droplet director distribution,  $S_s=0$ , and if the droplet directors are perfectly aligned along one direction,  $S_s=1$ . The relationship between  $S_s$  and the reduced field  $e$  is<sup>2</sup>

$$S_s = \frac{1}{4} + \frac{3(e^2+1)}{16e^2} + \frac{3(3e^2+1)(e^2-1)}{32e^3} \ln \left| \frac{e+1}{e-1} \right| . \quad (9)$$

The film order associated with each reduced field is also indicated in Figure 1. Surprisingly, application of reduced fields up to 1.0, which corresponds to  $S_s=0.67$ , has very little impact on the film cross-section for  $kR>30$ . Put another way, even though there is a substantial amount of director reorientation by the field, the transmitted light intensity is only weakly effected. For large  $kR$ , then, the voltage threshold should be much sharper.

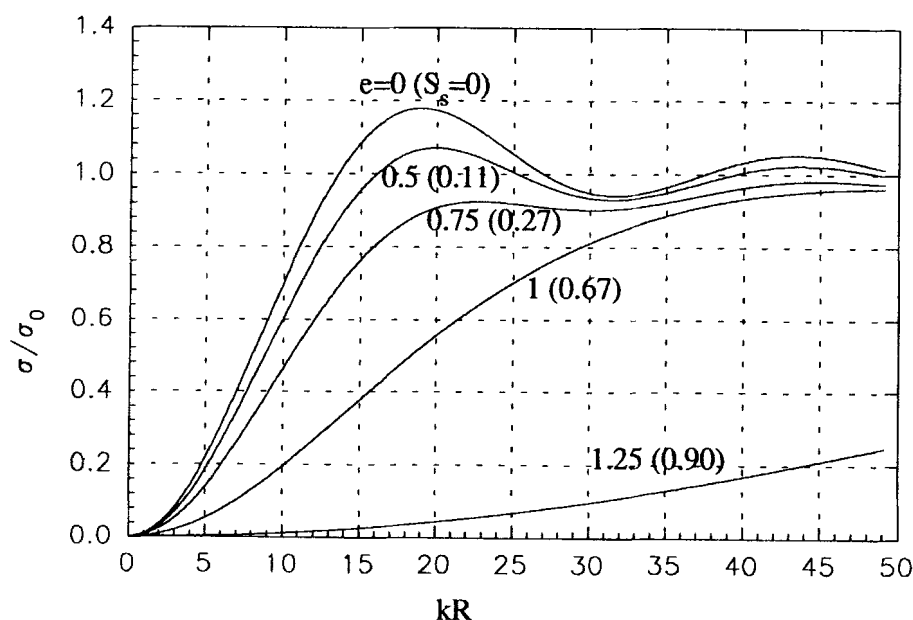


FIGURE 1 Film-averaged scattering cross-section vs.  $kR$  for various reduced fields (the film order parameter is given in parentheses).

## EXPERIMENT

PDLC samples were made with 50% E7 liquid crystal and 50% of the ultraviolet-cureable Norland optical adhesive NO65, sandwiched between ITO-coated glass. 10  $\mu\text{m}$  glass fiber spacers were used to control sample thickness. 10  $\mu\text{m}$  spacers were chosen so that the transmittance of the samples would be a few percent in the off state. The uv curing intensity was adjusted to obtain a range of droplet sizes<sup>6</sup>. Droplet sizes were measured with scanning electron microscopy. The curing intensity and droplet size for the five samples studied are given in Table I.

TABLE I

Sample number	1	2	3	4	5
UV power ( $\text{mW}/\text{cm}^2$ )	1.17	1.92	3.25	5.96	12.4
Droplet radius ( $\mu\text{m}$ )	1.3	1.1	0.8	0.6	0.3
$V_{10}$ (volt)	4	6	0	3	10
$V_{90}$ (volt)	9	11	12	15	22
Turn-on voltage range ( $V_{90}-V_{10}$ ) (volt)	5	5	12	12	12

For detailed measurements of the transmittance versus voltage, a multilane argon laser and a He-Ne laser were used to get a spectral range of 458nm to 633nm with 4 wavelengths. In order to get a broader spectral range for more detailed study of the wavelength dependence of the transmittance, a Lambda 4B UV/VIS spectrophotometer was employed. The samples were electrically switched with a 300hz sine wave. The transmitted light was collected by a photodetector whose collection half-angle was less than 1 degree.

## RESULTS AND DISCUSSION

Figures 2 and 3 show representative voltage response curves at the four laser wavelengths for the samples with droplets of radii 0.3  $\mu\text{m}$  and 1.3  $\mu\text{m}$ , respectively. For the 0.3  $\mu\text{m}$  sample, Figure 2 shows the transmittance to be a monotonically increasing function of the wavelength. This was also found true for the 0.6  $\mu\text{m}$  and

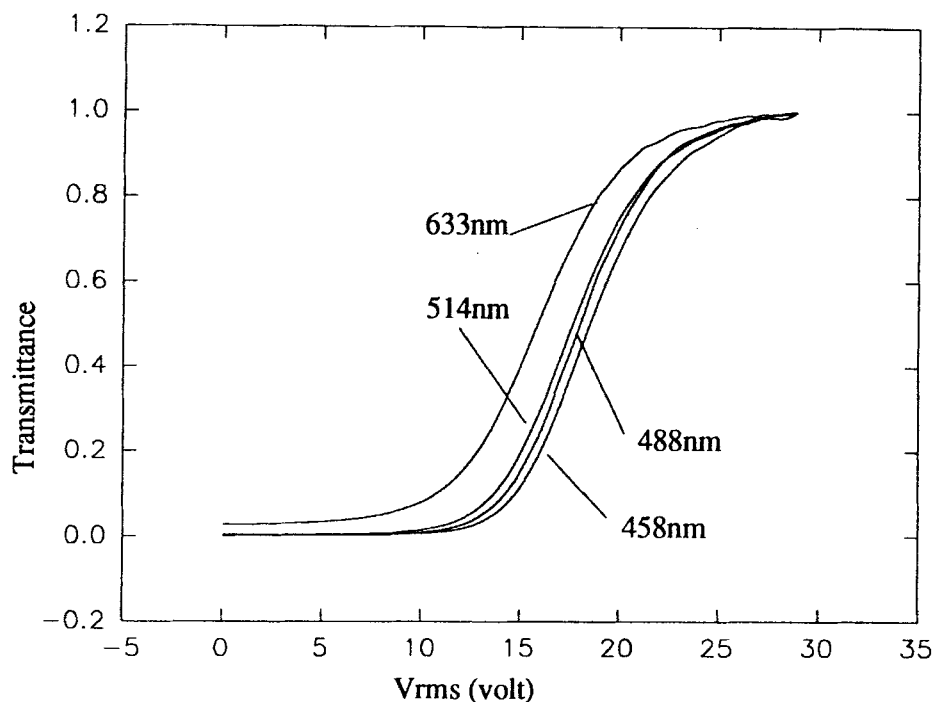


FIGURE 2 voltage response of transmittance at various wavelengths for  $0.3\ \mu\text{m}$  droplet sample.

$0.8\ \mu\text{m}$  samples. However, the  $1.1\ \mu\text{m}$  and  $1.3\ \mu\text{m}$  droplets were less scattering toward the blue in the off state; but with increasing voltage, they also became less scattering at the longer wavelengths.

As one would expect, the smaller droplets required a higher switching voltage. In addition, the smaller droplets had a much broader turn-on region (Table I). (The turn-on region is defined here as the difference in voltage between that required for 10% transmission,  $V_{10}$ , and 90% transmission,  $V_{90}$ .) As evidenced by Figures 2 and 3, the larger droplets have a much sharper voltage threshold as anticipated from the model. Regardless of which wavelength was scattered more strongly in the off-state, a sample always reached 90% transmission at a lower voltage,  $V_{90}$ , for the longest wavelength. For this reason,  $V_{90}$  was found to be a strong function of the wavelength. For example, for the  $0.3\ \mu\text{m}$  sample, there was nearly a 3 volt difference (16%) in  $V_{90}$  between red and blue light.

To study the dependence of transmittance on wavelength in more detail, we measured the transmittance of each sample with the spectrophotometer with no

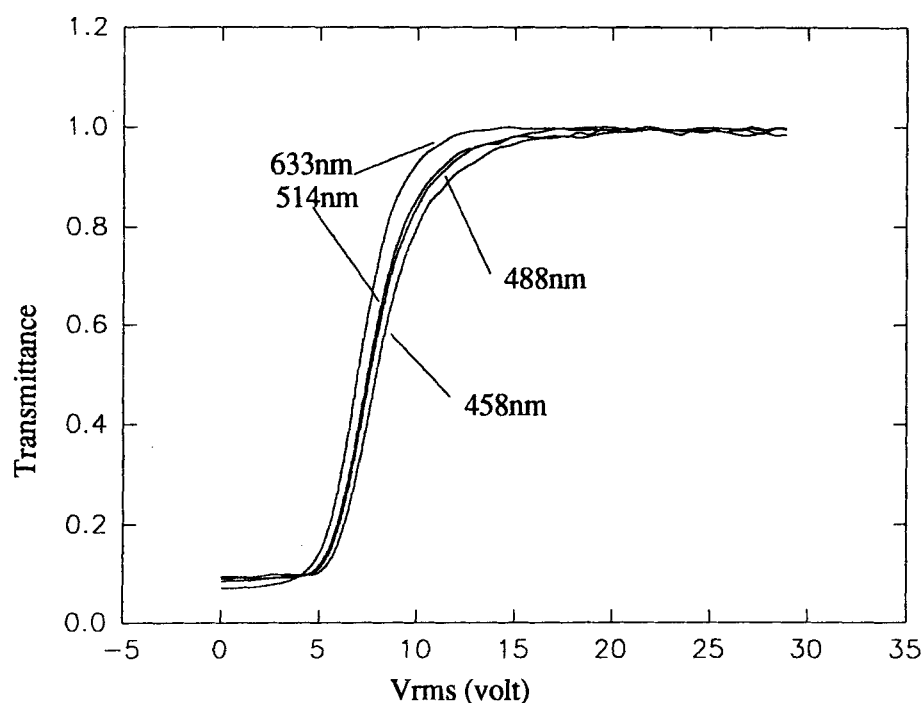


FIGURE 3 Voltage response of transmittance at various wavelengths for  $1.3\ \mu\text{m}$  droplet sample.

external voltage applied. The transmittance of the two samples with the largest droplets were also measured with different applied voltages.

According to Equation 1, the total scattering cross-section should be proportional to the logarithm of the transmittance. Figures 4 and 5 show  $-\ln(T)$  vs inverse wavelength for the  $1.1\ \mu\text{m}$  and  $1.3\ \mu\text{m}$  samples, respectively. These figures should be compared with the model prediction (Figure 1). Qualitatively, the agreement appears quite good. As predicted, the effect of the applied field is to destroy the peaks in the cross-section, eventually producing a monotonic dependence on wavenumber. The peaks in the zero field cross-section are more pronounced for the model; this probably results from a distribution of droplet sizes in the sample weakening the peaks.

Based on the AD model, the location of the primary maxima in the absence of a field should correspond to  $kR \approx 19$ . This gives predicted radii of  $1.2\ \mu\text{m}$  and  $1.4\ \mu\text{m}$  for the samples in Figures 4 and 5 respectively, in close agreement with the SEM values of  $1.1\ \mu\text{m}$  and  $1.3\ \mu\text{m}$ .

Combining the zero field results for all droplet sizes allows determination of the



scattering cross-section over the range  $3 < kR < 25$ . To convert the transmittance data to an effective cross-section, it is necessary to normalize the logarithm of the transmittance by dividing by  $\rho d$ . The droplet density  $\rho$  can be related to the volume fraction  $\eta$  of liquid crystal in the droplets:

$$\eta = \frac{4}{3}\pi R^3 \rho \quad (10)$$

$\eta$  is not known very precisely because an undetermined amount of liquid crystal remains behind in the polymer during the phase separation process. From SEMs of the larger droplets  $\eta$  was estimated to be in the neighborhood of 0.3 with rather large uncertainty. Estimates of 0.3 have also been obtained from comparisons of the PDLC dielectric constant in the off and on states.<sup>7</sup> Rather than treating  $\eta$  as a known quantity, it was adjusted to produce a smooth curve of the cross-section versus  $kR$  (Figure 6). Again, the main features of the cross-section agree with the AD prediction of Figure 1. In particular, the normalized cross-section tends to

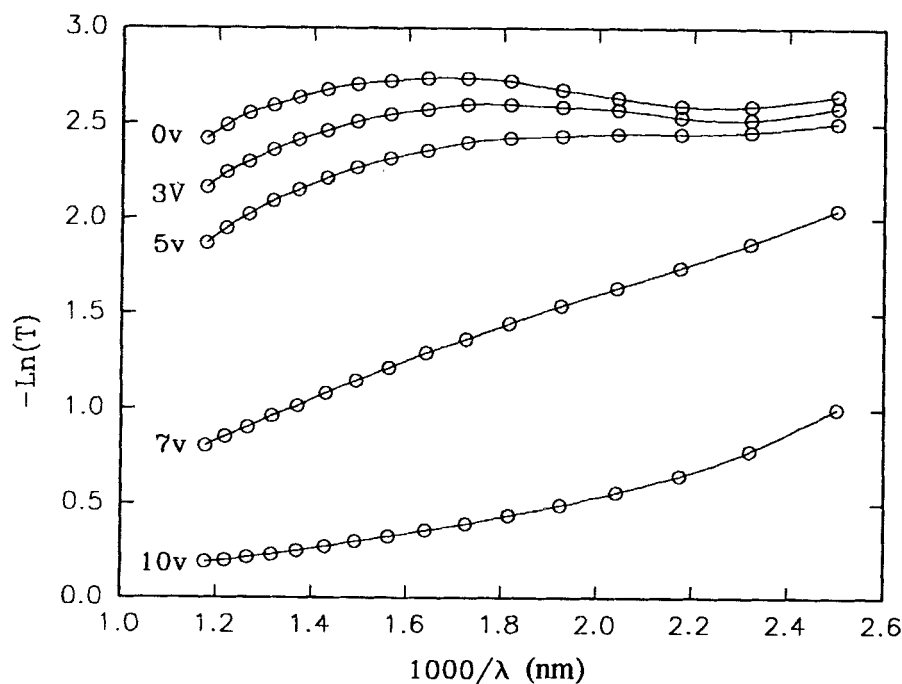


FIGURE 4 Frequency response at various applied voltages for 1.1  $\mu\text{m}$  droplet sample.

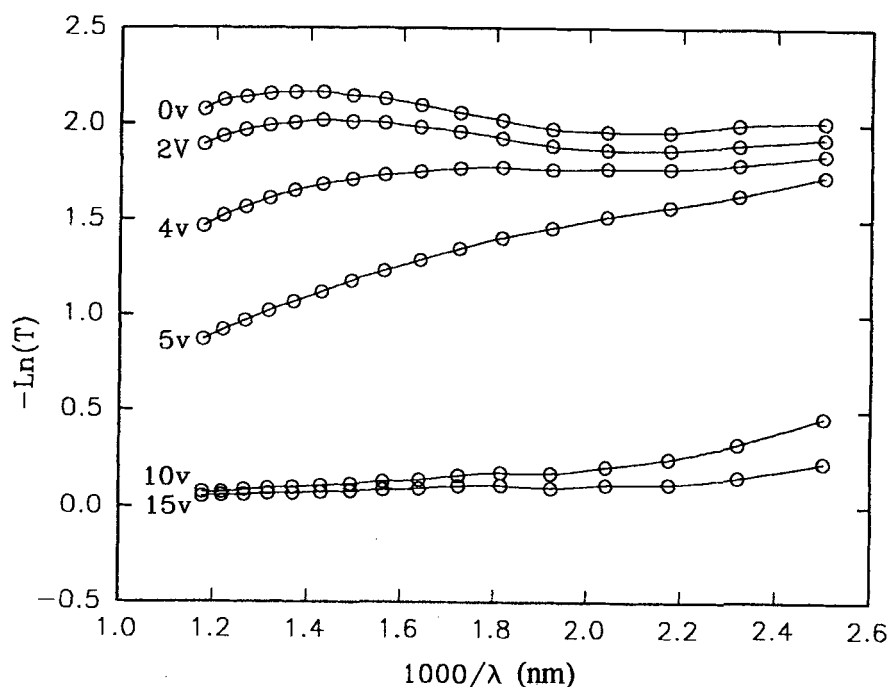


FIGURE 5 Frequency response at various applied voltages for 1.3  $\mu\text{m}$  droplet sample.

zero as  $kR \rightarrow 0$ , and is a monotonically increasing function of  $kR$  below  $kR=19$ . The cross-section saturates close to the geometrical cross-section.

The value of  $\eta$  used for each sample is shown in Figure 6. With the exception of the  $0.3\mu\text{m}$  droplets, for which  $\eta=0.5$ , the values are close to 0.3 in accord with the other observations mentioned above. For the  $0.3\mu\text{m}$  droplets, an  $\eta$  of 0.5 suggests that all of the liquid crystal has ended up in the droplets, which is highly unlikely. Another possible explanation is that Equation 1, which assumes a random distribution of droplet centers, begins to break down when  $d/R$  gets too large. We have performed some preliminary simulations which suggest that this may indeed be the case.

## CONCLUSIONS

We have studied the wavelength dependence of the light transmitted by PDLC films when the droplet size is comparable to, or larger than the wavelength of the incident radiation. The results of this study are in good agreement with the

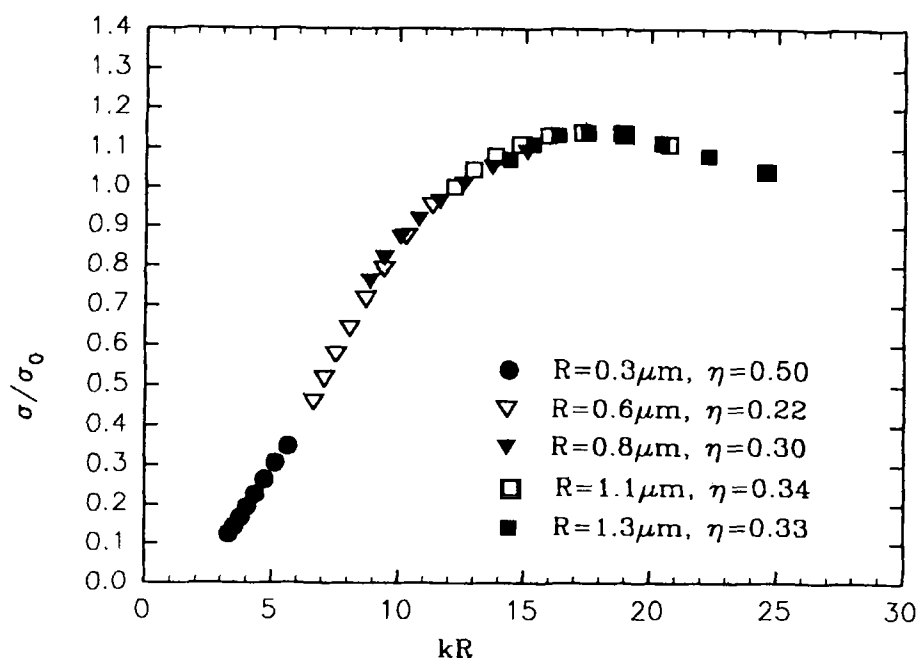


FIGURE 6 Scattering cross-section for various droplet size samples with zero applied voltage.

anomalous diffraction model. In particular, the droplet scattering cross-section saturates at approximately the geometrical cross-section when  $kR \geq 15$ . Most PDLCS that are used for display applications satisfy this criterion. Also, we have found that the position of the primary maximum in the cross-section can be used to get an excellent estimate of the mean droplet size.

The exponential decay law appears to give a good description of the attenuation of the incident intensity for the 50/50 NO65/E7 system, provided that the sample thickness is not too large compared to the droplet radius. We are currently studying this effect of film thickness on the transmittance in more detail, both theoretically and empirically. Also, it is perhaps surprising that a scattering cross-section based on isolated (i.e. non-interacting) scatterers should work so well at droplet volume fractions in the neighborhood of 0.3. Further work on the effects of droplet concentration are needed to clarify this issue.

### ACKNOWLEDGEMENTS

This research was supported in part by the National Science Foundation under the Science and Technology Center ALCOM DMR89-20147, and by the DARPA National Center for Integrated Photonics Technology Contract #MDA972-90-C-0037.

### REFERENCES

1. S.Zumer and J.W.Doane, Phys.Rev.A **34**, 3373 (1986).
2. S.Zumer, Phys.Rev.A **37**, 4006 (1988).
3. S.Zumer, A.Golomme and J.W.Doane, J.Opt.Soc.Am.A **6**, 403(1989).
4. P.Palfy-Muhoray, B.J.Frissen, J.Kelly and H.J.Yuan, SPIE **1105**, 33 (1989).
5. J.Kelly and P.Palfy-Muhoray, ALCOM Symposium Series **1**, 1(1991).
6. A.M.Lackner, J.D.Margrum, E.Ramos, and K.-C.Lim, SPIE **1080**, 53 (1989).
7. J.Kelly and D.Seekola, unpublished results.